Freezing of a Disorder Induced Spin Liquid with Strong Quantum Fluctuations

Xiao Hu,[1] Daniel M. Pajerowski,[2] Depei Zhang,[1] Andrey A. Podlesnyak⊙,[2] Yiming Qiu⊙,[3] Qing Huang,[4] Haidong Zhou,[4] Israel Klich,[1] Alexander I. Kolesnikov⊙,[2] Matthew B. Stone⊙,[2] and Seung-Hun Lee⊙[1,*]

[1]*Department of Physics, University of Virginia, Charlottesville, Virginia 22904, USA*
[2]*Neutron Scattering Division, Oak Ridge National Laboratory, Oak Ridge, Tennessee 37831, USA*
[3]*NIST Center for Neutron Research, National Institute of Standards and Technology, Gaithersburg, Maryland 20899, USA*
[4]*Department of Physics and Astronomy, University of Tennessee, Knoxville, Tennessee 37996, USA*

$Sr_2CuTe_{0.5}W_{0.5}O_6$ is a square-lattice magnet with superexchange between $S = \frac{1}{2} Cu^{2+}$ spins mediated by randomly distributed Te and W ions. Here, using sub-K temperature and 20 μeV energy resolution neutron scattering experiments we show that this system transits from a gapless disorder-induced spin liquid to a new quantum state below $T_f = 1.7(1)$ K, exhibiting a weak frozen moment of $\langle S \rangle / S \sim 0.1$ and low energy dynamic susceptibility, $\chi''(\hbar\omega)$, linear in energy which is surprising for such a weak freezing in this highly fluctuating quantum regime.

One of the most intriguing and elusive states of matter are quantum spin liquids (QSLs). Their features include spin and charge fractionalization and they have a possible application to topological quantum computing. Such states, envisioned and coined in Anderson's paper [1], exhibit zero-point fluctuations that prevent conventional magnetic order. Since this first description, the subject grew in importance suggesting a relation to superconductivity [2,3], the fractional quantum Hall effect [4] and topological order [5,6]. Experimental efforts to find QSLs have been focused on geometrically frustrated (GF) magnets where spins cannot order due to competing interactions [7]. Theoretical interest has also grown substantially after the establishment of stable QSLs in exactly solvable lattice models such as Kitaev's honeycomb model [8]. The works on the subject are detailed in a number of reviews [9,10]. While promising candidates for QSLs behavior have been GF quantum magnets [11–15], introduction of random local fields and other types of disorder in frustrated magnets have also been suggested to stabilize "glassy" QSL phases [16–19], further expanding theoretical efforts [18,20–23], and experimental search for QSLs into bond-disordered materials [17,24–26], which is the type of disorder considered in this Letter.

Despite the efforts over 30 years, an experimental identification of a true gapless QSL ground state has not been conclusively established. A crucial obstacle for experimentally establishing a QSL is that many candidates freeze at very low temperatures. For example, α-RuCl$_3$ orders at 7 K [12] and NiGa$_2$S$_4$ freezes below 8.5 K [27]. Theoretically, it has been shown that local coupling to the environment may result in local freezing leading to glassy behavior of QSL models [16]. Local freezing into metastable states can be favored entropically over remaining in

the QSL state. It is unknown whether such freezing is a salient feature to be expected of typical spin liquid (SL) candidates. Such systems are considered to be in the SL state for temperatures (T) below the Curie-Weiss temperature Θ_{CW}, however it is an open question whether as T approaches absolute zero they will exhibit some freezing or remain in the spin liquid state. A major experimental difficulty of approaching this regime is that most SL candidates have small values of $|\Theta_{CW}|$, making observation of potential spin freezing experimentally inaccessible.

$Sr_2CuTe_{0.5}W_{0.5}O_6$ offers a good model system to search for a disorder-induced spin liquid (SL) with strong quantum fluctuations. In this system the quantum spins of Cu^{2+} ions form a square lattice. Despite the presence of strong antiferromagnetic interactions indicated by $\Theta_{CW} = -71$ K [26], bond-disorder induced by random distribution of Te and W ions suppresses magnetic order. Here, we stress that there is no site disorder at the magnetic Cu sites. The bond disorder induced by mixing Te and W ions still keeps the Cu^{2+} ions strongly coupled, while changing the dominant coupling from the one between nearest neighboring Cu^{2+} ions (in the case of Te) to the one between the second nearest Cu^{2+} ions (in the case of W). Previous experiments did not observe freezing at T's well below $|\Theta_{CW}|$. In particular, a muon spin-relaxation (μSR) study reported that the spin correlations remain entirely dynamic down to 19 mK [26]. Interestingly, neutron scattering studies show that the dynamic spin correlations in the SL phase exhibit collective spin-wave-like excitations over the entire magnetic band [28]. Furthermore, the specific heat measurements exhibit an anomaly where a nearly linear in T specific heat below $\sim$7 K changes, upon further cooling, into quadratic behavior with T below $\sim$1.5 K [24].

This quadratic behavior may signal a transition from a SL into a frozen state. The puzzling nature of these experimental results calls for, considering the fact that the μSR is a local probe, a careful study using an experimental tool that directly probes the spatial and temporal spin correlations to understand the low temperature properties of this SL candidate.

Here, we report experimental evidence for freezing and existence of Goldstone-like modes in $Sr_2CuTe_{0.5}W_{0.5}O_6$ at low temperatures. Experimental evidence comes from time-of-flight (TOF) neutron scattering (NS) measurements with an extreme energy resolution of the half-width-at-half-maximum (HWHM) of $\Delta\hbar\omega_{HWHM} = 20~\mu$eV, down to sub-K temperatures. Our results show that this system exhibits freezing below $T_f \sim 1.7(1)$ K even though the frozen moment is very small, $\langle S \rangle / S \sim 0.1$. Below T_f the imaginary part of the dynamical susceptibility, $\chi''(\hbar\omega)$, behaves linearly with energy transfer $\hbar\omega$ for $\hbar\omega < k_B T_f$, where k_B is the Boltzmann constant, with the characteristic spin relaxation rate increasing with decreasing temperatures. The spatial spin correlations are two dimensional and short range with an in-plane correlation length of $\xi = 8.4(9)$Å $\sim \sqrt{2}d_{NN}$, where d_{NN} is the distance between nearest neighbor spins. In the SL state above T_f, the spatial spin correlations have the same nature at low energies as in the frozen state, i.e., short range and two dimensional. On the other hand, $\chi''(\hbar\omega)$ behaves as $\tan^{-1}(\hbar\omega/\Gamma_{min})$ at low energies indicating the presence of a distribution of the spin relaxation rate with the lower limit energy Γ_{min}. Γ_{min} behaves as a power law with temperature, $\Gamma_{min}/|J| = (k_B T/|J|)^\alpha$, with $\alpha = 1.3(1)$. These results tell us that $Sr_2CuTe_{0.5}W_{0.5}O_6$ transits from a gapless disorder-induced SL to a new quantum state below $\sim 1.7(1)$ K, exhibiting a weak frozen moment and $\chi''(\hbar\omega) \propto \hbar\omega$ for $\hbar\omega < k_B T_f$ consistent with Halperin-Saslow-like excitations.

The TOF NS experiments were performed on an 8 g powder sample of $Sr_2CuTe_{0.5}W_{0.5}O_6$. We performed the experiments with three different neutron incident energies E_i, using two different spectrometers at the Spallation Neutron Source (SNS) located at the Oak Ridge National Laboratory; $E_i = 1.55$ and 3.32 meV were used at the Cold Neutron Chopper Spectrometer (CNCS) [29] to focus on low energy excitations, and $E_i = 45$ meV at the Fine-Resolution Fermi Chopper Spectrometer (SEQUOIA) [30] to probe high energy excitations up to the top of the magnetic energy band.

Figure 1(a) shows contour maps of the NS cross section $S(Q, \hbar\omega)$ as a function of momentum transfer Q and $\hbar\omega$, acquired at 0.25 K with $E_i = 1.55$ and 3.32 meV, and at 5 K with $E_i = 45$ meV. The $E_i = 45$ meV data are shown only down to ~ 3 meV which corresponds to ~ 35 K and the magnetic excitations above 3 meV are expected to be similar at 5 and 0.25 K. The figure shows that the magnetic excitations extend from at least 0.05 meV up to 20 meV. The intensity was normalized to obtain $S(Q, \hbar\omega)$ in an
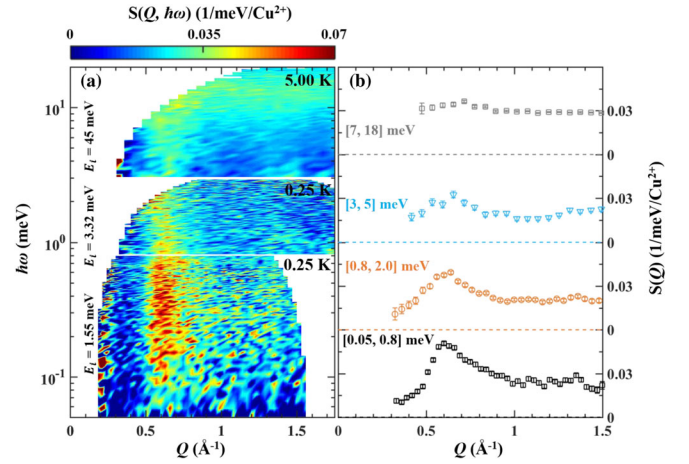

FIG. 1. Inelastic neutron scattering data of $Sr_2CuTe_{0.5}W_{0.5}O_6$. (a) Color contour maps of $S(Q, \hbar\omega)$ measured with $E_i = 1.55$ meV (bottom), 3.32 meV (middle), and 45 meV (top). (b) $S(Q) = \int S(Q, \hbar\omega) d(\hbar\omega) / \int d(\hbar\omega)$, for four different $\hbar\omega$-integration ranges. The dashed lines represent the zero value of the corresponding constant-$\hbar\omega$ cuts.

absolute unit of $1/$meV/Cu^{2+} by comparing the nuclear Bragg reflections to the calculated nuclear structure factors [31,32]. The total signal from 0.05 to 20 meV, $\int_{BZ} \int_{0.05~meV}^{20~meV} S(Q, \hbar\omega)/[f(Q)]^2 d(\hbar\omega) dQ / \int_{BZ} dQ$, where $f(Q)$ is the Cu^{2+} magnetic form factor, was estimated to be 0.5(1) which is consistent with the sum rule for the isotropic quantum spin of $\frac{2}{3}S(S+1) = 0.5$.

As shown in the Figs. 1(b) and 1(b), for $\hbar\omega \lesssim 7$ meV the magnetic excitations exhibit a prominent peak at $Q \sim 0.6$ Å^{-1}. On the other hand, for $\hbar\omega \gtrsim 7$ meV the magnetic excitations are almost featureless in Q, which is due to the Van Hove singularity of the top of the magnetic energy band from a powder sample. These overall features of $S(Q, \hbar\omega)$ can be understood as being due to a powder-averaged spin wave spectrum in a long range ordered magnetic state, similarly to the $S(Q, \hbar\omega)$ reported for the two mother compounds Sr_2CuTeO_6 [33,34] and Sr_2CuWO_6 [35,36], both of which exhibit long range order long range at low temperatures.

If we closely examine the data, however, we notice a peculiar feature. Figure 1(b) shows the constant $\hbar\omega$ cuts of $S(Q, \hbar\omega)$, $S(Q)$, for four different energy ranges. For $\hbar\omega \gtrsim 0.8$ meV, $S(Q)$ shows long ranged spin-wave-like features, exhibiting a prominent peak at $Q \sim 0.6$ Å^{-1} for $\hbar\omega \lesssim 7$ meV and being almost featureless for $\hbar\omega \gtrsim 7$ meV. Note that $S(Q)$ for both $3 \leq \hbar\omega \leq 5$ meV (blue triangles) and $0.8 \leq \hbar\omega \leq 2$ meV (orange circles) are more or less symmetric about $Q \sim 0.6$ Å^{-1}. On the other hand, the $S(Q)$ for $0.05 \leq \hbar\omega \leq 0.8$ meV (black squares) is strikingly asymmetric in Q. This indicates that the very low energy spin fluctuations are due to low-dimensional dynamic spin fluctuations. The low-dimensional low-energy spin fluctuations may hold a key in understanding
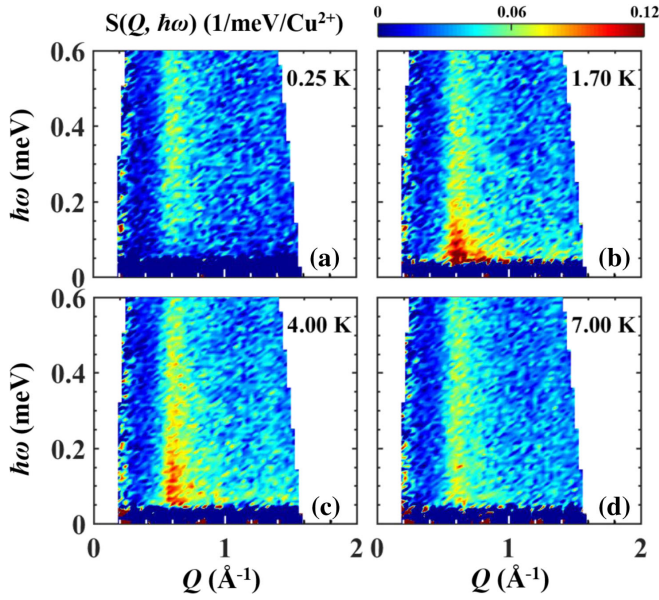
FIG. 2. Low energy spin fluctuations of $Sr_2CuTe_{0.5}W_{0.5}O_6$. Color contour maps of $S(Q, \hbar\omega)$, obtained with $E_i = 1.55$ meV, measured at (a) 0.25 K, (b) 1.70 K, (c) 4.00 K, and (d) 7.00 K. The background was determined by an algorithm using the detailed balance condition, $S(Q, -\hbar\omega) = e^{-\hbar\omega/k_B T} S(Q, \hbar\omega)$, and subtracted from the raw data to get $S(Q, \hbar\omega)$.
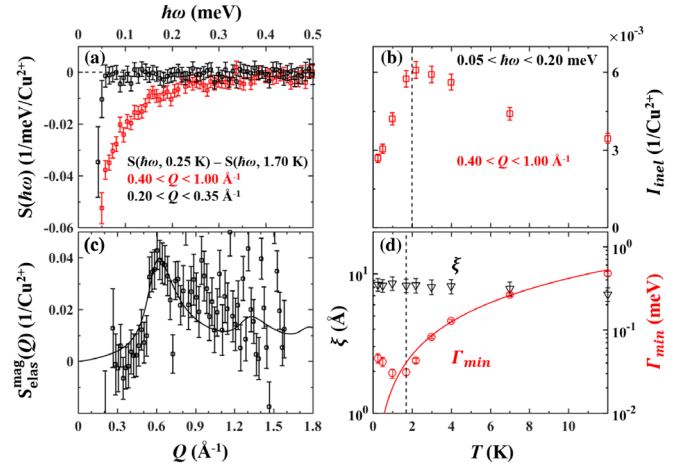

FIG. 3. (a) $S(\hbar\omega) = \int S(Q, \hbar\omega)dQ$, obtained with $E_i = 1.55$ meV at 0.25 K is shown after $S(\hbar\omega)$ at 1.7 K $\sim T_f$ was subtracted. The Q-integration range for the red squares was 0.4 Å^{-1} < Q < 1.0 Å^{-1} including $q_m = (\frac{1}{2}, 0, 0)$, while that for the black squares was 0.2 Å^{-1} < Q < 0.35 Å^{-1} below q_m. (b) The red squares represent $I_{inel} = \tilde{S} \equiv \int_{0.4 \text{ Å}^{-1}}^{1.0 \text{ Å}^{-1}} \int_{0.05 \text{ meV}}^{0.2 \text{ meV}} S(Q, \hbar\omega)/[f(Q)]^2 d(\hbar\omega)dQ$. (c) The elastic magnetic scattering cross section, $S_{elas}^{mag}(Q, 0.25 \text{ K}) = \int_{-0.02 \text{ meV}}^{0.02 \text{ meV}} S(Q, \hbar\omega)d(\hbar\omega)$ measured at 0.25 K, after background subtraction. The black curve is the fit discussed in the text. (d) The red circles are Γ_{min} as a function of temperature. The red solid line is discussed in the text. The black triangles are the correlation length ξ.

the reported anomalous low temperature magnetic properties [24–26]. The focus of this Letter is how the low energy excitations below $\hbar\omega \sim 0.8$ meV evolve as a function of temperature down to sub-K.

The TOF measurements with $E_i = 1.55$ meV providing $\Delta\hbar\omega_{HWHM} = 20$ μeV were performed at nine different temperatures from 0.25 to 12 K. Figure 2 shows the $S(Q, \hbar\omega)$ for four T's, 7, 4, 1.7, and 0.25 K. At all T's, the low energy excitations are dominated by the gapless streak centered at $Q \sim 0.6$ Å^{-1}. The measured scattering intensity indicates that the system is gapless down to the lowest energy $\hbar\omega \sim 0.05$ meV that can be accessed by $\Delta\hbar\omega_{HWHM} = 20$ μeV. Upon cooling from 7 to 1.7 K, $S(Q, \hbar\omega)$ increases in strength for $\hbar\omega < 0.3$ meV, and the spectral weight gradually shifts to lower energies. Surprisingly, however, a close look at the 0.25 K data shown in Fig. 2(a) shows that below 0.2 meV $S(Q, \hbar\omega)$ becomes weak upon further cooling from 1.7 to 0.25 K. This change can be more clearly seen with the Q-integrated intensity difference between 1.7 and 0.25 K, [see Fig. 3(a)]. The depletion of $S(Q, \hbar\omega)$ at low energies is typically a signature of spin freezing.

In order to investigate how the low energy spin fluctuations evolve upon cooling, we plotted $\tilde{S} \equiv \int_{0.4 \text{ Å}^{-1}}^{1.0 \text{ Å}^{-1}} \int_{0.05 \text{ meV}}^{0.2 \text{ meV}} S(Q, \hbar\omega)/[f(Q)]^2 d(\hbar\omega)dQ$ over a range of Q and $\hbar\omega$ covering the prominent low energy peak centered at 0.6 Å^{-1} as a function of T. In Fig. 3(b), as T decreases from 12 to 2 K, $\tilde{S}$ get gradually stronger. Upon

further cooling from 2 K, however, $\tilde{S}$ gradually weaken, transferring to the elastic channel [see Fig. 3(c)]. This indicates that the spins indeed freeze below $T_f \sim 1.7(1)$ K. These findings starkly contradict the previous μSR study [26] that reported a QSL state down to 19 mK. How could μSR not be able to detect the spin freezing? The clue comes from the fact that the spin freezing is very weak: as shown in Fig. 3(b), the frozen spectral weight is $\Delta\tilde{S} = \tilde{S}(2 \text{ K}) - \tilde{S}(0.25 \text{ K}) \cong 0.003$ per Cu^{2+}. Thus, below T_f only 0.6% out of the total spectral weight of the isotropic quantum spin that is $\frac{2}{3}S(S + 1) = 0.5$ is frozen and the rest is fluctuating.

To study the nature of the weak spin freezing, we plotted the elastic magnetic scattering cross section, $S_{elas}^{mag}(Q, 0.25 \text{ K}) = \int_{-0.02 \text{ meV}}^{0.02 \text{ meV}} S(Q, \hbar\omega)d(\hbar\omega)$ measured at 0.25 K, after background subtraction. Here, background was determined by averaging similar elastic $S_{elas}(Q)$ measured at three different T's, 4, 7, and 12 K above T_f, to increase the statistics. As shown in Fig. 3(c), $S_{elas}^{mag}(Q, 0.25 \text{ K})$ exhibits an asymmetric broad peak at $Q \sim 0.6$ Å^{-1} similarly to the low energy gapless excitations shown in Fig. 2. This implies that the static correlations of the frozen spins are basically the same as the dynamic correlations of the fluctuating moments. The black line is the fit to a phenomenological Lorentzian function with a two-dimensional correlation length of $\xi = 12(6)$ Å that

will be explained in detail later. The large error for ξ is due to the weak signal and resulting poor statistics.

To investigate the nature of the critical spin fluctuations at low energies, we have generated constant-Q and constant-$\hbar\omega$ cuts from $S(Q, \hbar\omega)$ taken at nine different T's around T_f. $S(\hbar\omega)$ was then converted to $\chi''(\hbar\omega)$ using the fluctuation dissipation theorem. The resulting $S(Q)$ and $\chi''(\hbar\omega)$ for four different T's are shown in Figs. 4(a) and 4(b), respectively.

First, note that $S(Q)$ exhibits a prominent asymmetric peak with a maximum at $Q \approx 0.6$ Å^{-1} that corresponds to $Q = (\frac{1}{2}, 0, 0)$, a sharp edge at lower Q's, and a long tail at higher Q's. There is another peak at $Q \approx 1.3$ Å^{-1} that corresponds to $Q = (\frac{1}{2}, 1, 0)$. Thus, the low energy spin fluctuations have a characteristic antiferromagnetic wave vector of $q_m = (\frac{1}{2}, 0, 0)$. For a quantitative analysis of the spin dynamical correlation, we fit $S(Q)$ to the product of the independent lattice-Lorentzian functions [32,37],

$$\frac{d\sigma(\mathbf{Q})}{d\Omega} \propto |F_m^\perp(\mathbf{Q})|^2 \prod_\alpha \frac{\sinh(\xi_\alpha^{-1})}{\cosh(\xi_\alpha^{-1}) - \cos[(\mathbf{q_m} - \mathbf{Q}) \cdot \hat{\mathbf{r}}_\alpha]}. \quad (1)$$

Here, $F_m^\perp(\mathbf{Q}) = f(Q)\Sigma_\nu \mathbf{M}_\nu^\perp e^{-i\mathbf{Q}\cdot\mathbf{r}_\nu}$, where $\mathbf{M}_\nu$ and $\mathbf{r}_\nu$ are the staggered magnetic moment and the position of a Cu^{2+} ion at the site ν, respectively, and $f(Q)$ is the Cu^{2+} magnetic form factor. ξ_α and $\hat{r}_\alpha$ are the spin-correlation length and the unit cell lattice vector along the crystallographic axis ($\alpha = a, b, c$), respectively. The scattering cross section was convoluted with the instrumental resolution to fit the data. In the fitting, we used two different correlation lengths, an isotropic in-plane correlation length $\xi = \xi_a = \xi_b$ and an out-of-plane correlation length ξ_c. The fitting results are shown as the solid lines in Fig. 4(a). For all the low temperatures considered, ξ_c was negligible. Furthermore, as shown in Fig. 3(d), the in-plane correlation

length ξ is very short, $\xi = 8.4(9)$ Å $\sim \sqrt{2}d_{NN}$ at 0.25 K. ξ gets slightly shorter above T_f: $\xi = 7.1(8)$ Å at 12 K. Thus, the critical spin fluctuations at low temperatures have very short two-dimensional correlations that fall off quickly when the distance between the quantum spins goes beyond the distance between the second nearest neighbors.

Figure 4(b) shows $\chi''(\hbar\omega)$. At 7 K $\ll |\Theta_{CW}|$, $\chi''(\hbar\omega)$ gradually increases with increasing $\hbar\omega$. Upon cooling down to 1.7 K 1.7 K $\approx T_f$, $\chi''(\hbar\omega)$ softens, i.e., the spectral weight gradually shifts to lower energies. This low energy behavior is expected for a spin liquid since the energy scale of a spin liquid is $k_B T$ where $k_B \approx 0.086$ meV/K is the Boltzmann constant. For a quantitative analysis, we compare $\chi''(\hbar\omega)$ to a phenomenological function, $\chi''(\hbar\omega) \propto \tan^{-1}(\hbar\omega/\Gamma_{min})$, that assumes a broad distribution of spin relaxation rates with the lower limit of Γ_{min} [38]. Figure 3(d) shows the resulting Γ_{min} in a log scale as a function of T. The red line is a fit to a function, $\Gamma_{min}/|J| = (k_B T/|J|)^\alpha$, with an energy scale of the magnetic interactions, $|J| = 9(2)$ meV, and a power, $\alpha = 1.3(1)$. The value of $|J|$ being close to the previously reported value of the dominant magnetic interaction [28], $J_2 \sim -9$ meV, and α being close to 1 support our interpretation that Sr$_2$CuTe$_{0.5}$W$_{0.5}$O$_6$ is in a SL state above T_f. Upon further cooling below T_f, however, low-energy spin degrees of freedom get depleted in the frozen state [see Fig. 3(b)] where $\chi''(\hbar\omega) \propto \hbar\omega$ up to $k_B T_f \approx 0.15$ meV, as shown in Fig. 4(b). $\chi''(\hbar\omega) \propto \hbar\omega$ for $\hbar\omega < k_B T_f$ is consistent with $C(T) \propto T^2$ for $k_B T < k_B T_f$ [24].

The exploration of disorder induced SLs brings with it new challenges. Disorder can induce magnetic frustration without the presence of geometric frustration, and can lead to new RG (renormalization group) fixed points featuring local excitations as well as unusual dynamical exponents
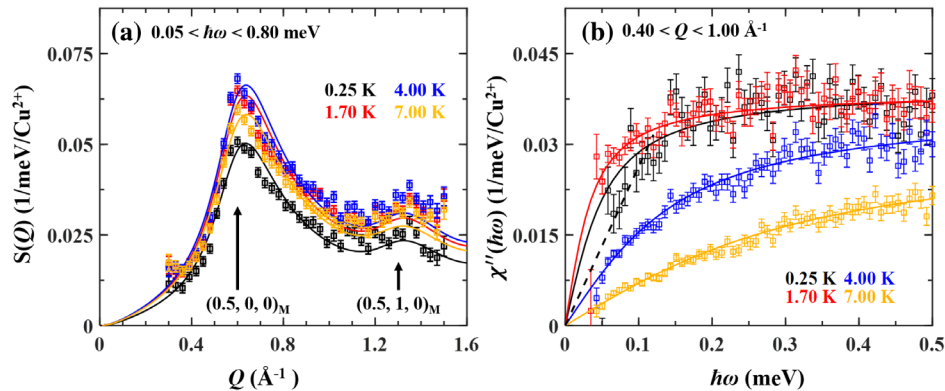

FIG. 4. Q and $\hbar\omega$ dependences of low energy spin fluctuations in Sr$_2$CuTe$_{0.5}$W$_{0.5}$O$_6$. (a) $S(Q) = \int_{0.05 \text{ meV}}^{0.80 \text{ meV}} S(Q, \hbar\omega)d(\hbar\omega)/$ $\int_{0.05 \text{ meV}}^{0.80 \text{ meV}} d(\hbar\omega)$, at 0.25 K (black squares), 1.70 K (red), 4.00 K (blue), and 7.00 K (orange). The color solid lines are discussed in the text. (b) $\chi''(\hbar\omega) = (1 - e^{-\hbar\omega/k_B T})S(\hbar\omega)$ where $S(\hbar\omega) = \int_{0.40 \text{ Å}^{-1}}^{1.00 \text{ Å}^{-1}} S(Q, \hbar\omega)d(Q)/\int_{0.40 \text{ Å}^{-1}}^{1.00 \text{ Å}^{-1}} d(Q)$, at 0.25 K (black), 1.70 K (red), 4.00 K (blue), and 7.00 K (orange). The color solid lines are described in the text. The black dashed line represents the linear $\hbar\omega$ dependence of $\chi''(\hbar\omega)$ up to ~ 0.15 meV.

[17–19,39]. Moreover, disorder can both facilitate a liquid state as well as facilitate freezing. Here, we uncover a freezing phenomenon of a disorder-induced spin liquid in which, remarkably, development of an extremely small frozen moment induces substantial changes in low T properties. Our findings of freezing below 1.7 K tell us that the previous reported C_v anomaly at 1.5 K [24] is indeed intrinsic to the system due to the freezing transition. The frozen moment, however, is very small, $\langle S \rangle / S \sim 0.1$, and 99.4% out of the total spectral weight $\frac{2}{3} S(S+1)$ is fluctuating. Despite the small frozen moment, the behavior of $\chi''(\hbar\omega)$ changes through the transition. In the SL state above T_f, $\chi''(\hbar\omega) \propto \tan^{-1}(\hbar\omega/\Gamma_{\min})$ with $\Gamma_{\min} \propto (k_B T)^\alpha$ with $\alpha = 1.3(1)$. In the weakly frozen state below T_f, $\chi''(\hbar\omega) \propto \hbar\omega$ for $\hbar\omega < k_B T_f$. These results are consistent with C_v being linear just above T_f and being quadratic below T_f [24].

In a previous experimental study the state above T_f was regarded as a valence-bond glass (VBG) [24,40,41]. The magnetic excitations, however, do not exhibit any singlet-to-triplet-excitations characteristic of valence bonds [see Fig. 1(a) and Refs. [1–5,28]]. Rather, the magnetic excitations at high energies resemble spin-wave excitations of the ordered state of Sr_2CuWO_6, even though the excitations are smeared in energy [28,36]. Thus, we believe it is more appropriate to call the state of $Sr_2CuTe_{0.5}W_{0.5}O_6$ above T_f a disorder-induced glassy SL rather than VBG. Below T_f, $\chi''(\hbar\omega) \propto \hbar\omega$ and $C_v(T) \propto T^2$. Such behavior is consistent with linearly dispersing modes with density of states $\rho(\omega) \propto \omega^{D-1}$ where D is the magnetic dimensionality. In systems with rotationally invariant interactions, such modes appear as Goldstone modes that are a consequence of a spontaneous symmetry breaking into a long range ordered state. However, such linearly dispersing modes can appear even in symmetry broken states without long range order, and such modes in Heisenberg spin glasses are called Halperin-Saslow (HS) modes [42,43]. These suggest that the frozen state is a quantum analog of a spin jam state, a glassy state typical for nondilute frustrated magnets [44]. The spin jam is a distinct state from an ordinary spin glass of diluted magnets. The low energy spin dynamics of a spin jam is governed by the HS modes while those of a spin glass is by localized two-level energy states [42–44], leading to different memory effects [45]. The main assumptions in the Halperin-Saslow theory are the presence of some freezing as well as nonvanishing spin stiffness. [42]. While the Halperin-Saslow scenario is an appealing direction to explain the experimental observations, it is unknown how effective such a mechanism can be in our system where the frozen moment is very small, $\langle S \rangle / S \sim 0.1$. This presents a theoretical challenge to fully understand the mechanism of the freezing of the disorder-induced SL and the possible extension of HS theory into this new highly fluctuating quantum regime.

*Corresponding author.
 shlee@virginia.edu

[1] P. W. Anderson, Mater. Res. Bull. **8**, 153 (1973).
[2] P. W. Anderson, Science **235**, 1196 (1987).
[3] G. Baskaran, Z. Zou, and P. W. Anderson, Solid State Commun. **63**, 973 (1987).
[4] V. Kalmeyer and R. B. Laughlin, Phys. Rev. Lett. **59**, 2095 (1987).
[5] S. A. Kivelson, D. S. Rokhsar, and J. P. Sethna, Phys. Rev. B **35**, 8865 (1987).
[6] X. G. Wen, Phys. Rev. B **40**, 7387 (1989).
[7] A. Ramirez, *Geometrical frustration, in Handbook of Magnetic Materials*, 1st ed., edited by K. H. J. Buschow (Elsevier Science, Amsterdam, 2001), Vol. 13.
[8] A. Kitaev, Ann. Phys. (Amsterdam) **321**, 2 (2006).
[9] L. Savary and L. Balents. Rep. Prog. Phys. **80**, 016502 (2017).
[10] C. Broholm, R. J. Cava, S. A. Kivelson, D. G. Nocera, M. R. Norman, and T. Senthil, Science **367**, eaay0668 (2020).
[11] T.-H. Han, J. S. Helton, S. Chu, D. G. Nocera, J. A. Rodriguez-Rivera, C. Broholm, and Y. S. Lee, Nature (London) **492**, 406 (2012).
[12] A. Benerjee, J. Yan, J. Knolle, C. A. Bridges, M. B. Stone, M. D. Lumsden, D. G. Mandrus, D. A. Tennant, R. Moessner, and S. E. Nagler, Science **356**, 1055 (2017).
[13] S.-H. Do, S.-Y. Park, J. Yoshitake, J. Nasu, Y. Motome, Y. S. Kwon, D. T. Adroja, D. J. Voneshen, K. Kim, T.-H. Jang, J.-H. Park, K.-Y. Choi, and S. Ji, Nat. Phys. **13**, 1079 (2017).
[14] S. Chillal, Y. Iqbal, H. O. Jeschke, J. A. Rodriguez-Rivera, R. Bewley, P. Manuel, D. Khalyavin, P. Steffens, R. Thomale, A. T. M. Nazmul Islam, J. Reuther, and B. Lake, Nat. Commun. **11**, 2348 (2020).
[15] S.-H. Lee, C. Broholm, W. Ratcliff, G. Gasparovic, Q. Huang, T. H. Kim, and S.-W. Cheong, Nature (London) **418**, 856 (2002).
[16] L. Savary and L. Balents, Phys. Rev. Lett. **118**, 087203 (2017).
[17] S.-H. Baek, H. W. Yeo, S.-H. Do, K.-Y. Choi, L. Janssen, M. Vojta, and B. Buchner. Phys. Rev. B **102**, 094407 (2020).
[18] L. Liu, H. Shao, Y.-C. Lin, W. Guo, and A. W. Sandvik, Phys. Rev. X **8**, 041040 (2018).
[19] L. Liu, W. Guo, and A. W. Sandvik, Phys. Rev. B **102**, 054443 (2020).
[20] H. Kawamura and K. Uematsu, J. Phys. Condens. Matter **31**, 504003 (2019).
[21] H. Kawamura, K. Watanabe, and T. Shimokawa, J. Phys. Soc. Jpn. **83**, 103704 (2014).

[22] K. Uematsu and H. Kawamura, J. Phys. Soc. Jpn. **86,** 044704 (2017).

[23] K. Watanabe, H. Kawamura, H. Nakano, and T. Sakai, J. Phys. Soc. Jpn. **83,** 034714 (2014).

[24] M. Watanabe, N. Kurita, H. Tanaka, W. Ueno, K. Matsui, and T. Goto, Phys. Rev. B **98,** 054422 (2018).

[25] O. Mustonen, S. Vasala, K. P. Schmidt, E. Sadrollahi, H. C. Walker, I. Terasaki, F. J. Litterst, E. Baggio-Saitovitch, and M. Karppinen, Phys. Rev. B **98,** 064411 (2018).

[26] O. Mustonen, S. Vasala, E. Sadrollahi, K. P. Schmidt, C. Baines, H. C. Walker, I. Terasaki, F. J. Litterst, E. Baggio-Saitovitch, and M. Karppinen, Nat. Commun. **9,** 1085 (2018).

[27] S. Nakatsuji, Y. Nambu, H. Tonomura, O. Sakai, S. Jonas, C. Broholm, H. Tsunetsugu, Y. Qiu, and Y. Maeno, Science **309,** 1697 (2005).

[28] V. M. Katukuri, P. Babkevich, O. Mustonen, H. C. Walker, B. Fak, S. Vasala, M. Karppinen, H. M. Ronnow, and O. V. Yazyev, Phys. Rev. Lett. **124,** 077202 (2020).

[29] G. Ehlers, A. A. Podelsnyak, J. L. Niedziela, E. B. Iverson, and P. E. Sokol, Rev. Sci. Instrum. **82,** 085108 (2011).

[30] G. E. Granroth, A. I. Kolesnikov, T. E. Sherline, J. P. Clancy, K. A. Ross, J. P. Ruff, B. D. Gaulin, and S. E. Nagler, J. Phys. Conf. Ser. **251,** 012058 (2010).

[31] G. Xu, Z. Xu, and J. M. Tranquada, Rev. Sci. Instrum. **84,** 083906 (2013).

[32] I. A. Zaliznyak and S.-H. Lee, *Neutron scattering with 3-axis spectrometer, in Modern Techniques for Characterizing Magnetic Materials*, edited by Y. Zhu (Kluwer, Boston/Dordrecht/London, 2004).

[33] T. Koga, N. Kurita, M. Avdeev, S. Danilkin, T. J. Sato, and H. Tanaka, Phys. Rev. B **93,** 054426 (2016).

[34] P. Babkevich, V. M. Katukuri, B. Fak, S. Rols, T. Fennell, D. Pajic, H. Tanaka, T. Pardini, R. R. P. Singh, A. Mitrushchenkov, O. V. Yazyev, and H. M. Ronnow, Phys. Rev. Lett. **117,** 237203 (2016).

[35] S. Vasala, M. Avdeev, S. Danilkin, O. Chmaissem, and M. Karppinen, J. Phys. Condens. Matter **26,** 496001 (2014).

[36] H. C. Walker, O. Mustonen, S. Vasala, D. J. Voneshen, M. D. Le, D. T. Adroja, and M. Karppinen, Phys. Rev. B **94,** 064411 (2016).

[37] S. Ji, E. J. Kan, M.-H. Whangbo, J.-H. Kim, Y. Qiu, M. Matsuda, H. Yoshida, Z. Hiroi, M. A. Green, T. Ziman, and S.-H. Lee, Phys. Rev. B **81,** 094421 (2010).

[38] J. A. Mydosh, *Spin Glasses: An Experimental Introduction* (Taylor & Francis London, 1993).

[39] W. Hong, L. Liu, C. Liu, X. Ma, A. Koda, X. Li, J. Song, W. Yang, J. Yang, P. Cheng, H. Zhang, W. Bao, X. Ma, D. Chen, K. Sun, W. Guo, H. Luo, A. W. Sandvik, and S. Li, Phys. Rev. Lett. **126,** 037201 (2021).

[40] M. Tarzia and G. Biroli, Europhys. Lett. **82,** 67008 (2008).

[41] R. R. P. Singh, Phys. Rev. Lett. **104,** 177203 (2010).

[42] B. I. Halperin and W. M. Saslow, Phys. Rev. B **16,** 2154 (1977).

[43] D. Podolsky and Y. B. Kim, Phys. Rev. B **79,** 140402 (2009).

[44] I. Klich, S.-H. Lee, and K. Iida, Nat. Commun. **5,** 3497 (2014).

[45] A. Samarakoon, T. J. Sato, T. Chen, G. W. Chern, J. Yang, I. Klich, R. Sinclair, H. Zhou, and S.-H. Lee, Proc. Natl. Acad. Sci. U.S.A. **113,** 11806 (2016).